A hybrid embedded discrete fracture model for simulating tight porous media with complex fracture systems

Xu, Jianchun
Sun, Baojiang
Chen, Bailian

To be published in: Journal of Petroleum Science and Engineering

DOI to publisher's version: 10.1016/j.petrol.2018.10.094

Permalink to record: http://permalink.lanl.gov/object/view?what=info:lanl-repo/lareport/LA-UR-18-30867

Accepted Manuscript

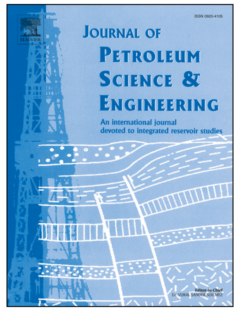

A hybrid embedded discrete fracture model for simulating tight porous media with complex fracture systems

Jianchun Xu, Baojiang Sun, Bailian Chen

PII: S0920-4105(18)30962-8

DOI: https://doi.org/10.1016/j.petrol.2018.10.094

Reference: PETROL 5457

To appear in: *Journal of Petroleum Science and Engineering*

Received Date: 10 April 2018

Revised Date: 17 October 2018

Accepted Date: 26 October 2018

Please cite this article as: Xu, J., Sun, B., Chen, B., A hybrid embedded discrete fracture model for simulating tight porous media with complex fracture systems, *Journal of Petroleum Science and Engineering* (2018), doi: https://doi.org/10.1016/j.petrol.2018.10.094.

A Hybrid Embedded Discrete Fracture Model for Simulating Tight Porous Media with Complex Fracture Systems

Jianchun Xu[1]*, Baojiang Sun[1]*, Bailian Chen[2]

1.School of Petroleum Engineering, China University of Petroleum (East China), Qingdao, China, 266580

2. Computational Earth Science Group, Los Alamos National Laboratory, Los Alamos, NM 87545, USA

*Correspondence to: 20170048@upc.edu.cn/sunbj1128@vip.126.com

Abstract

Numerical simulation considering complex fracture networks in tight oil reservoir becomes a hot issue during these years. Recently, embedded discrete fracture model (EDFM) shows great advantages over the DFM approaches in both calculation efficiency and simplicity of simulation workflow. EDFM has been widely used in tight oil/gas natural energy or enhanced oil recovery (EOR) development. If a large number of small-scale natural fractures exist in reservoir, the calculation efficiency of EDFM method may decrease. In this paper, a new hybrid simulation model combining the EDFM and dual porosity (DP) model is proposed. The large-scale fractures are dealt with EDFM method while small scale fractures are dealt with DP model. Considering the low permeability of matrix, transient transfer between matrix and natural fracture is considered. The proposed hybrid model is validated compared with the local grid refinement (LGR) model and EDFM-MINC model, and the difference between transient transfer and pseudo-steady-state transfer effect on production is presented. Finally, two test cases are presented, and the sensitivity of some key parameters are investigated. Result shows that the new simulation model has higher calculation efficiency than LGR and EDFM-MINC models. Meanwhile, it honors a good accuracy. The pseudo-steady-state transfer between matrix and natural fracture leads to big error in tight oil production performance analysis both in single phase and two phases flow. Low matrix permeability and big matrix size increase the production difference between pseudo-steady-state transfer and transient transfer models. The proposed model can simulate reservoirs considering stochastic permeability distribution.

Keywords

Numerical simulation; Discrete fracture model; Naturally fractured tight oil reservoir; Transient transfer; Stochastic permeability

1. Introduction

Advances in numerical simulation technology are promoting global interest in unconventional resources development such as tight oil/gas. Hydraulic fracturing is always employed for tight porous media such as shale gas/tight oil to achieve high production rate [1, 2, 3]. Reasonable and efficiency numerical simulation tool plays an important role for hydrocarbon production design. Various numerical models have been proposed to simulate oil and gas flow in subsurface [4, 5]. Generally, two approaches are used to characterize and model naturally fractured system: Dual-porosity/ dual-permeability (DP/DK) models and discrete fracture model (DFM) [6].

Dual porosity model was proposed by Barenblatt and Zheltov (1960) firstly [7] and then widely improved and used in simulation of naturally fractured reservoirs (NFRs) [8, 9, 10]. DP/DK model assumes the representative volume element (RVE) exists and uses relatively uniform properties to characterize matrix and naturally fracture [11]. Low computational cost is an important advantage for DP/DK model. The shape factor is a key parameter to calculate the flux between matrix and fracture [12]. Various format shape factors are proposed [9, 10, 13, 14, 15, 16, 17, 18, 19, 20, 21, 22, 23, 24, 25, 26, 27] using analytical or numerical methods. Commonly, there are two categories of shape factors: classical and time-dependent shape factors [21]. The classical shape factors are used widely in numerical simulation software like CMG and Eclipse. The classical shape factor assumes fracture and matrix transfer arrives the pseudo-steady. This assumption is validated only when the transient regime last short. While for tight porous media, transient transfer regime last long as the ultra-low permeability of matrix. Transient transfer flow should be considered between matrix and fracture [28, 29, 30].

To overcome the disadvantages of DP/DK model, DFM seems a better way to characterize the detail of complex fracture. Many scholars have done research on DFM [31, 32, 33, 34, 35, 36]. Unstructured grids always used in DFM model. Explicit processing of fractures needs large number of grids thus makes the simulation costly. During these years, embedded discrete fractured model (EDFM) shows great advantages in tight reservoir simulation. EDFM was proposed by Lee et al. [37, 38]. This model is described as a hierarchical approach to characterize multiple length-scale fractures. By comparison with the grid size, the short fractures are dealt with to enhance the matrix conductivity using analytical method. The boundary element method is used to calculate the medium length fractures contribution to matrix permeability. The long-scale fractures are modelled as discrete fracture model. A tensor permeability simulator should be used to simulate the enhanced matrix permeability tensor. Compared with DP model, EDFM is adequate to represent high anisotropy fractures [39]. Monifar et al. [40] extended EDFM to simulate IOR processes in naturally fractured reservoirs fractures. In their work, three connections are defined and explained in detail: connection between a fracture cell and its neighboring matrix grid, connection between two intersecting fracture cells and connection between two cell domains of an individual fracture. The calculation rules for connection transmissibility are determined. **Figure 1** shows the connections when using EDFM. Then the EDFM is improved for the simulation of unconventional oil/gas reservoirs [41, 42]. The natural fracture and hydraulic fracture can both taken as embedded discrete factures. After defining connections and calculating transmissibility in pre-processing code, the simulation is simple to performance using in-house simulators.

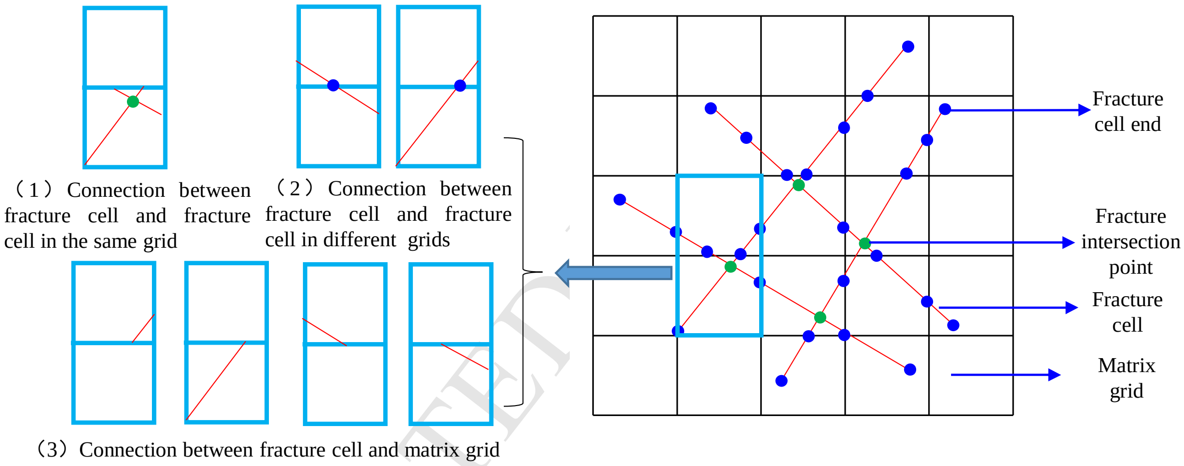

Figure 1. Connections in embedded discrete fracture model

Much improvement has been performed on EDFM. The geomechanics was considered that allows the simulation of stress-sensitive or fracture propagation [43, 44, 45]. The compositional model EDFM was developed for tight reservoirs [46, 47, 48]. Siripatrachai et al. (2017) highlighted the effect of capillary pressure in their simulation. The capillary pressure should be considered in both flow and phase behavior calculation [46]. Zuloaga-Molero et al. (2016) analyzed the CO_2 Huff-n-Puff performance in Bakken Formation. Different fracture geometries effect on oil production are discussed [47]. The CO_2-EOR was evaluated in detail and its good application prospect in tight oil development was proven [48]. When developing tight oil reservoirs, a large fracture network is beneficial to maximize well performance, the EDFM is widely used in hydraulic fracture simulation [49]. Recently, it is extended to unstructured grids including triangle mesh grids and coordinate grids [50, 51]. Another progress in EDFM is coupling it with multi-continuum model [52, 53]. Recently, the EDFM incorporates different porosity type media has been developed. Porosity types includes kerogen, inorganic matrix, micro fracture, and macro fracture. The transfer between different media uses pseudo-steady shape factor [52]. Wang et al. proposed a comprehensive model in which the EDFM was coupled with multiple interacting continua (MINC) [53]. The same method was used by coupling the DFM with the MINC [54].

After hydraulic fracturing, a complex hydraulic fracture system may exist. Fluids flow in different space, i.e, hydraulic fractures, natural fractures, and matrix [55]. So the simulation model must characterize the flow reasonable and the same for the coupling of transfer between different media.

Although many numerical models have confirmed that EDFM is a good method to model naturally fractured tight reservoirs [11]. Few have been presented to investigate the transient transfer behavior. Though MINC model can simulate transient transfer from matrix to fracture by dividing the matrix, it increases the Jacobian Matrix size which is time consuming. This is the basic motivation for our work. As porous flow happens in multiple length scale fractures, the flow coupling between different length scale space should be modelled. The EDFM is used to characterize the flow between large scale fracture hydraulic fracture and relatively small scale natural fractures. On the other hand, the transfer between matrix and natural fracture also need to be evaluated as the tight matrix permeability cause a long time of unsteady flow between them [28]. To our best knowledge, the simulation model and simulation performance has not been investigated when using the EDFM considering analytical transient transfer formula. In this paper, we will show a new workflow how to combine the transient transfer between natural fracture and matrix and EDFM to simulate the flow behavior of naturally fractured tight reservoirs with complex hydraulic fractures. The goal is to combine the advantages of EDFM and transient transfer shape factor and thus improve the computational efficiency of naturally fractured tight oil reservoir. Moreover, we make comparison between transient transfer and pseudo-steady-state shape factor and shows the error when using pseudo-steady-state shape factor in tight reservoir. The rest of this paper is organized as following. Section 2 describes the proposed physical model we focus on in detail. The physics significance is presented; Section 3 presents the mathematical model and the solution workflow is also showed for the model;

Section 4 shows the comparison of different numerical model to verify the new numerical simulation method. Calculation efficiency studies are conducted for different numerical schemes. Section 5 presents a number of test cases that contain different fracture geometries to benchmark the performances of the hybrid simulation method for multiphase flow. Some important parameters are analyzed.

2. Physical model

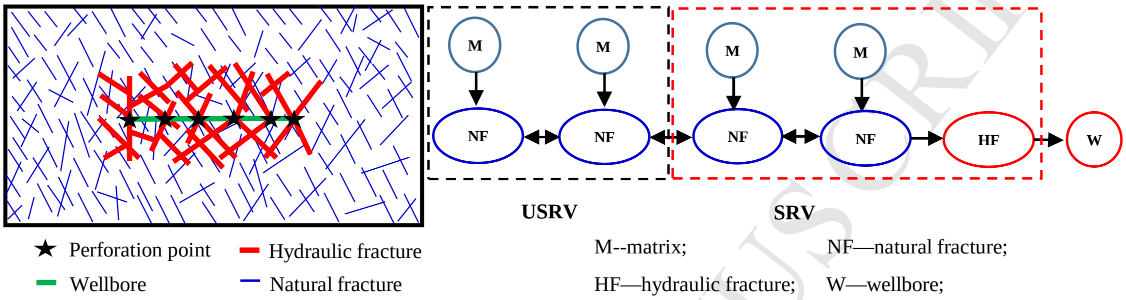

(1). fracture network **(2). transport among different media**

Figure 2. Schematic of physical model and transport between different media

Figure 2(1) shows the physical model. The green line indicates the horizontal well. Several perforation points distribute along the well and cause the hydraulic fracture after fracturing fluid is injected. The fracturing fluid is always non-Newtonian [56, 57]. The red lines present the complex hydraulic fractures with high conductivity. The hydraulic fracture network will dominate the flow dynamics in the production process. The blue lines are the natural fractures. Natural fractures always exist with low conductivity thus leads to low permeability of formation [55]. The natural fracture permeability is lower than hydraulic fractures. The zone with complex hydraulic fractures is named as Stimulated Reservoir Volume (SRV) while the outer region is un-Stimulated Reservoir Volume (USRV) [58]. **Figure 2(2)** shows the transport between different media. Fluids first flow into the wellbore from the SRV and then pressure spreads to USRV which causes flow within it. Next, the hybrid model will be established. In the model, the hydraulic fractures are modelled with EDFM methods while the matrix and natural fractures are modelled with DP model. The new numerical model is established based on the following assumptions: (1) three space system is considered from matrix to natural facture to hydraulic fractures; (2) the fluid flow along the matrix-natural fracture-hydraulic fracture-wellbore successively; (3) the flow is under isothermal condition; (4) flow is single or two phases. In the production stage for the well, the flow obeys Darcy's law; (5) the fluid is slightly compressible.

The viscosity and density change with the pressure.

3. Mathematical model

3.1 Two-phase flow

The two-phase flow is considered. The mass conservation equations for oil and water phases respectively are followed for fracture:

$$-\nabla\cdot\left(\rho_{\mathrm{of}} v_{\mathrm{of}}\right)+(\rho_{\mathrm{o}}u_{\mathrm{o}}^{*})_{\mathrm{m}}+q_{\mathrm{mo}}=\frac{\partial\left(\phi_{\mathrm{f}}\rho_{\mathrm{of}}S_{\mathrm{of}}\right)}{\partial t} \tag{1}$$

$$-\nabla\cdot\left(\rho_{\mathrm{wf}} v_{\mathrm{wf}}\right)+(\rho_{\mathrm{w}}u_{\mathrm{w}}^{*})_{\mathrm{m}}+q_{\mathrm{mw}}=\frac{\partial\left(\phi_{\mathrm{f}}\rho_{\mathrm{wf}}S_{\mathrm{wf}}\right)}{\partial t} \tag{2}$$

Where ϕ is porosity; ρ is density; q denotes the source and sink terms; u^{*} is the transfer flux between matrix and nature fracture; t is the time. For hydraulic fracture, the transfer term between matrix and fracture is ignored. The phase velocity can be expressed using Darcy's Law:

$$v_{\mathrm{f}}=-\frac{k_{\mathrm{f}}k_{\mathrm{r}}}{\mu_{\mathrm{f}}}\nabla p_{\mathrm{f}} \tag{3}$$

While in matrix, oil and water flow obeys the following equations:

$$-(\rho_{\mathrm{o}}u_{\mathrm{o}}^{*})_{\mathrm{m}}=\frac{\partial\left(\phi_{\mathrm{m}}\rho_{\mathrm{om}}S_{\mathrm{om}}\right)}{\partial t} \tag{4}$$

$$-(\rho_{\mathrm{w}}u_{\mathrm{w}}^{*})_{\mathrm{m}}=\frac{\partial\left(\phi_{\mathrm{m}}\rho_{\mathrm{wm}}S_{\mathrm{wm}}\right)}{\partial t} \tag{5}$$

The transfer between matrix and fracture is given by:

$$u^{*}=\frac{\alpha_{\mathrm{m}}k_{\mathrm{m}}k_{r}}{\mu}(p_{\mathrm{m}}-p_{\mathrm{f}}) \tag{6}$$

If the pseudo-steady-state shape factor is considered, as discussed in the **Introduction** part, a lot of shape factors can be chosen. Here, we use the shape factor proposed by Kazemi and Gilman (1993) [15]:

$$\alpha_{m}=\pi^{2}\left(\frac{1}{L_{x}^{2}}+\frac{1}{L_{y}^{2}}+\frac{1}{L_{z}^{2}}\right) \tag{7}$$

Where k is the permeability; L_x, L_y, L_z is the matrix size in x, y, z direction; μ is the viscosity of fluids; k_r is the relative permeability. The subscripts m, f, w, o, respectively, denote matrix, natural fracture, water and oil. If the transient transfer shape factor is considered, the shape factor proposed by Zimmerman et al. (1993) is used [14]:

$$\alpha_{\mathrm{munsteady}} = \alpha_{\mathrm{m}} \frac{\left(p_{\mathrm{i}} - p_{\mathrm{f}}\right)^2 - \left(p_{\mathrm{i}} - p_{\mathrm{m}}\right)^2}{2\left(p_{\mathrm{i}} - p_{\mathrm{m}}\right)\left(p_{\mathrm{m}} - p_{\mathrm{f}}\right)} \tag{8}$$

The following equations are required to form the mathematical model:

$$S_{\mathrm{of}} + S_{\mathrm{wf}} = 1 \tag{9}$$

$$p_{\mathrm{cowf}} = p_{of} - p_{wf} \tag{10}$$

$$S_{\mathrm{om}} + S_{\mathrm{wm}} = 1 \tag{11}$$

$$p_{\mathrm{cowm}} = p_{\mathrm{om}} - p_{\mathrm{wm}} \tag{12}$$

where S is the saturation and p_{c} is the capillary pressure. Also, the reasonable initial condition and boundary condition should be included.

3.2 Discretization method

The discretization method refers to conventional black oil reservoir model. Time is discretized using backward scheme. The fully-implicit discretization of the fracture and matrix are as follows:

$$\Delta T_{\mathrm{of}}^{n+1} \Delta p_{\mathrm{of}}^{n+1} + \lambda_{\mathrm{o}}^{n+1}(p_{\mathrm{om}}^{n+1} - p_{\mathrm{of}}^{n+1})V_{\mathrm{b}} + Q_{\mathrm{mo}}^{n+1} = \frac{V_{\mathrm{b}}}{\Delta t}[(\phi_{\mathrm{f}} \rho_{\mathrm{of}} S_{\mathrm{of}})^{n+1} - (\phi_{\mathrm{f}} \rho_{\mathrm{of}} S_{\mathrm{of}})^{n}] \tag{13}$$

$$\Delta T_{\mathrm{wf}}^{n+1} \Delta p_{\mathrm{wf}}^{n+1} + \lambda_{\mathrm{w}}^{n+1}(p_{\mathrm{wm}}^{n+1} - p_{\mathrm{wf}}^{n+1})V_{\mathrm{b}} + Q_{\mathrm{mw}}^{n+1} = \frac{V_{\mathrm{b}}}{\Delta t}[(\phi_{\mathrm{f}} \rho_{\mathrm{wf}} S_{\mathrm{wf}})^{n+1} - (\phi_{\mathrm{f}} \rho_{\mathrm{wf}} S_{\mathrm{wf}})^{n}] \tag{14}$$

$$-\lambda_{\mathrm{o}}^{n+1}(p_{\mathrm{om}}^{n+1} - p_{\mathrm{of}}^{n+1})V_{\mathrm{b}} = \frac{V_{\mathrm{b}}}{\Delta t}[(\phi_{\mathrm{m}} \rho_{\mathrm{om}} S_{\mathrm{om}})^{n+1} - (\phi_{\mathrm{m}} \rho_{\mathrm{om}} S_{\mathrm{om}})^{n}] \tag{15}$$

$$-\lambda_{\mathrm{w}}^{n+1}(p_{\mathrm{wm}}^{n+1} - p_{\mathrm{wf}}^{n+1})V_{\mathrm{b}} = \frac{V_{\mathrm{b}}}{\Delta t}[(\phi_{\mathrm{m}} \rho_{\mathrm{wm}} S_{\mathrm{wm}})^{n+1} - (\phi_{\mathrm{m}} \rho_{\mathrm{wm}} S_{\mathrm{wm}})^{n}] \tag{16}$$

$$S_{\mathrm{of}}^{n+1} + S_{\mathrm{wf}}^{n+1} = 1 \tag{17}$$

$$p_{\mathrm{cowf}}^{n+1} = p_{of}^{n+1} - p_{wf}^{n+1} \tag{18}$$

$$S_{\mathrm{om}}^{n+1} + S_{\mathrm{wm}}^{n+1} = 1 \tag{19}$$

$$p_{\mathrm{cowm}}^{n+1} = p_{\mathrm{om}}^{n+1} - p_{\mathrm{wm}}^{n+1} \tag{20}$$

where

$$T_{\mathrm{f}} = \rho \frac{k_{\mathrm{f}} k_{r} A}{\mu d} \tag{21}$$

$$\lambda = \alpha(\frac{k_m k_r \rho}{\mu})_m \tag{22}$$

V_b is the volume of grids; Q denotes the source and sink terms of mass. T_f is the transmissibility of fracture (commonly, the density ρ and viscosity μ are arithmetic averaged; $\frac{kA}{d}$ is harmonic averaged; k_r takes the value of up-wind).

3.3 Improvement of EDFM

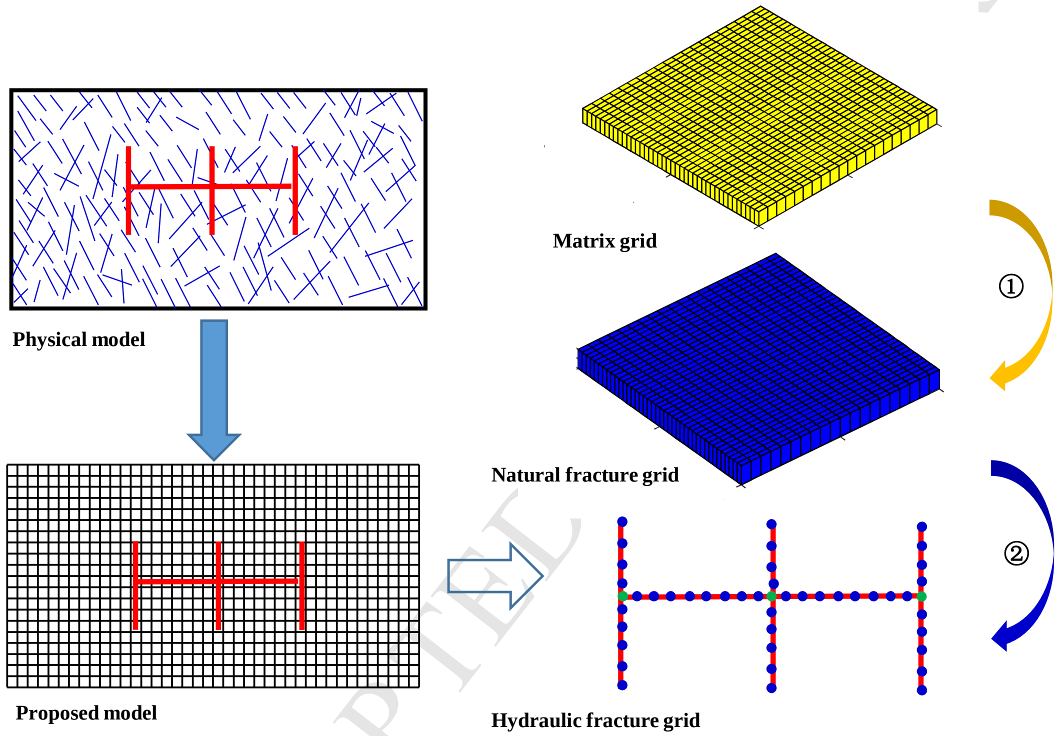

Figure 3. Improvement of EDFM

In general, EDFM always use Cartesian grid to discretize reservoir geology. As shown in Figure 1, hydraulic fractures are discretized by the Cartesian grid boundaries automatically. **Figure 3** shows a model which includes four hydraulic fractures (the red lines) and 185 natural fractures (the blue lines). In the new model, the matrix and natural fractures are taken as dual porosity media. The matrix and natural fracture grids are discretized by Cartesian grid and the hydraulic fractures are discretized as embedded discrete fractures. As can been seen, compared with the EDFM proposed before, the connection between hydraulic fracture and natural facture should be defined and the transmissibility should be calculated. This model is a hybrid model which combines the EDFM (to deal with hydraulic fractures) and DP (to deal with natural fractures and matrix) models. The freedom degrees contain the pressure and saturation for matrix cells, natural fracture cells and hydraulic fracture cells. As an improvement, there are three kinds of connections to redefine: (1) connection between natural fracture grid and hydraulic fracture grid; (2) connection between hydraulic grid belonging to different natural fracture grids; (3) connection of hydraulic fracture grid belonging to the same natural fracture grid.

Considering the hydraulic fracture segment, some new connections should be added to the mass conservation equation for fractures:

$$-\nabla\cdot\left(\rho_{\mathrm{f}}v_{\mathrm{f}}\right)V_{\mathrm{b}}+V_{\mathrm{b}}(\rho u^{*})_{\mathrm{m}}+Q_{\mathrm{m}}+q_{N}=V_{\mathrm{b}}\frac{\partial\left(\phi_{\mathrm{f}}\rho_{\mathrm{f}}S_{\mathrm{f}}\right)}{\partial t} \tag{23}$$

where q_N is given by

$$q_N = T_N \frac{k_r}{\mu}\rho\nabla p \tag{24}$$

$$T_N = \frac{A^N k^N}{d^N} \tag{25}$$

EDFM defined three Non-neighborhood connections [51]. For all three connections, the two-point flux approximation (TPFA) scheme is used for all connections [11, 54]. In the new model, the same method is used to calculate the transmissibility for the above three connections when considering hydraulic fracture, natural fracture, and matrix.

3.4 Solution

As shown in **Figure 3**, after the discretization of the geological model, some procedures should be obeyed as following:

(1) Define the matrix and natural fracture grids. Determine hydraulic fracture segments divided by natural fracture grid boundaries;

(2) Prepare the connections for matrix, natural fracture and hydraulic fracture domain.

(3) Generate the connection list. Each list contains the left domain, right domain and transmissibility. The transmissibility is calculated according to the method in section 3.3;

(4) Identify fracture segments intersected by a well and calculate the well index of the corresponding fracture control volumes; the Control Volume Function Approximation (CVFA) is employed to couple the well and hydraulic facture [59].

The calculation procedure of the program is shown in **Figure 4**. The new numerical simulator was developed based on the finite difference method and compiled on the basis of black-oil model. The code of the framework is programed by C++.

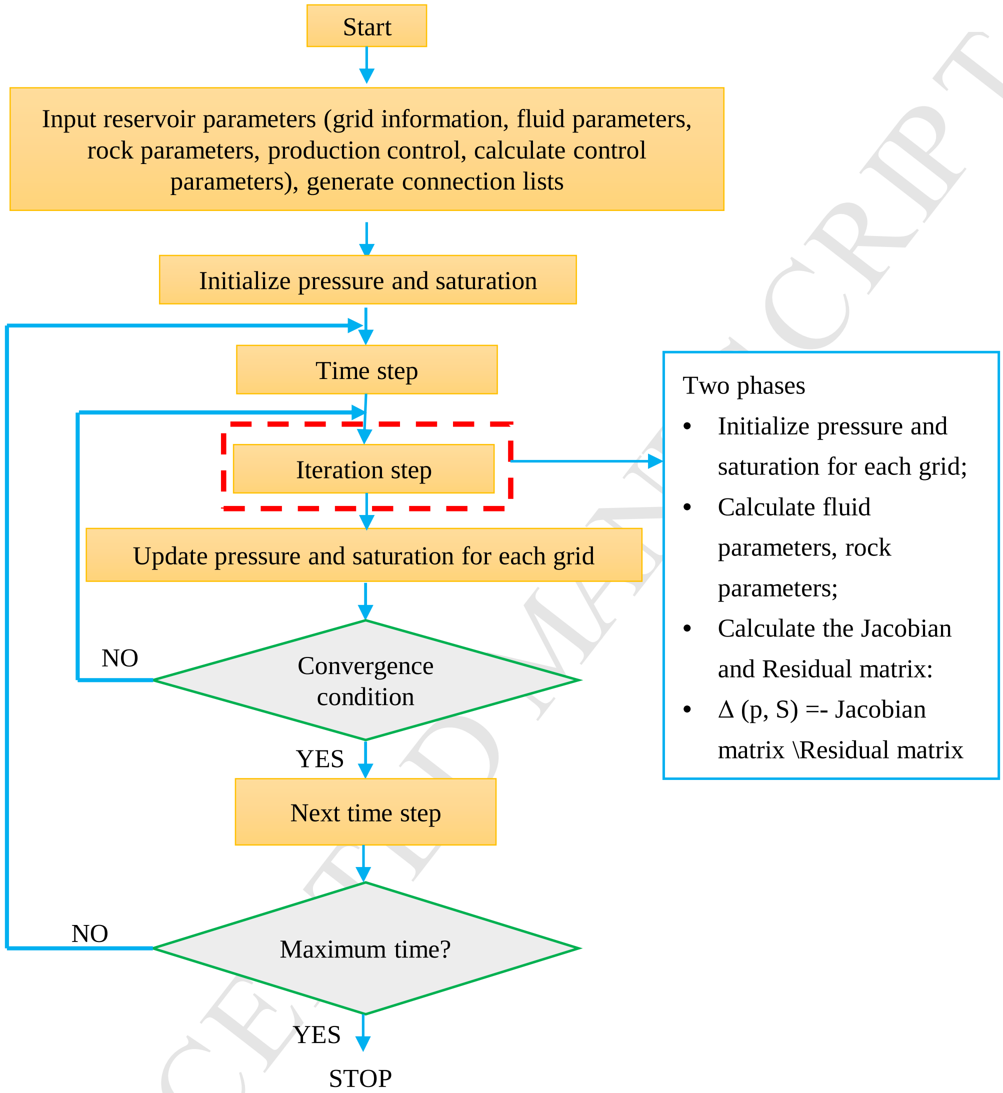

Figure 4. Framework of the Improved EDFM

4. Validation

We show a simple example to illustrate how to use the improved EDFM method for the simulation of multiphase flow. As shown in **Figure 5(1)**, the reservoir model contains 100 matrix blocks and one hydraulic fracture. The matrix block size is 10×10×10 m and each matrix block is surrounded by natural fractures. The proposed model is compared with three existing models. Four simulation cases (four simulation models) are set as follows:

① In the first simulation case, the local grid refinement (LGR) method is used for both natural fracture and hydraulic fractures. The total grid number is 171×171=29241. This model is treated as the basic model and is fully resolved. **Figure 5(1)** also presents the local refinement grids;
② In the second simulation case, the MINC model is coupled with EDFM [51]. Figure 6 shows a 2D physical model when MINC model is used. In the model, the matrix block is discretized by small volume element. Flux happens between the neighboring elements. Five volume elements of matrix block are divided in the simulation. Considering the grid system in Figure 5, the total calculation domain is 2657 including 11 hydraulic fracture domain, 441 natural fracture domain and 2205 matrix domain;

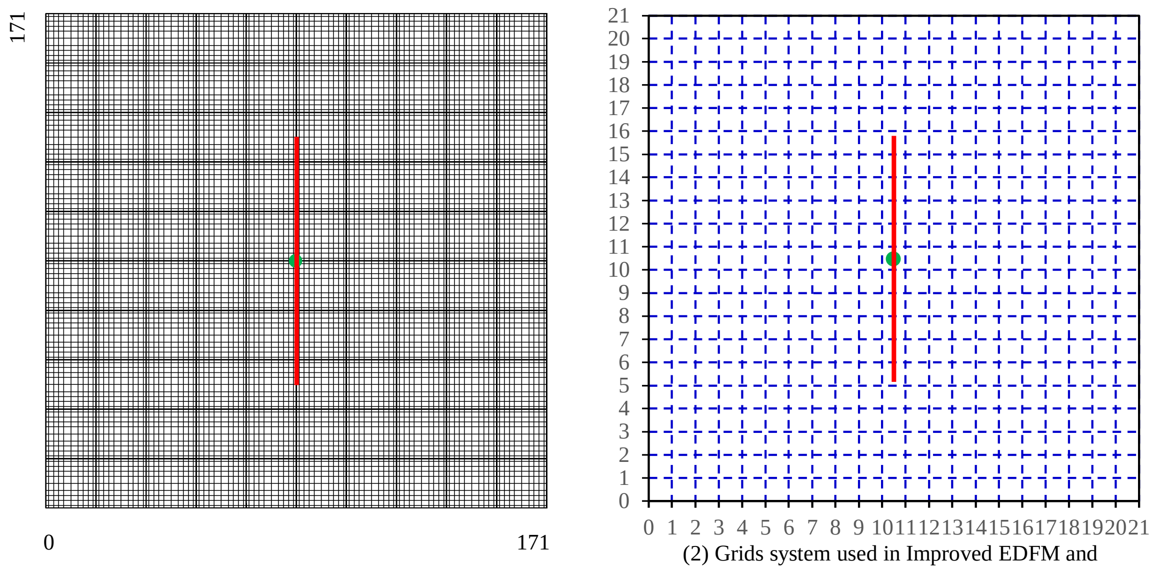

(1) Grids system used in LGR model

(2) Grids system used in Improved EDFM and EDFM+MINC model

Figure 5. Schematic of LGR model, Improved EDFM and MINC model

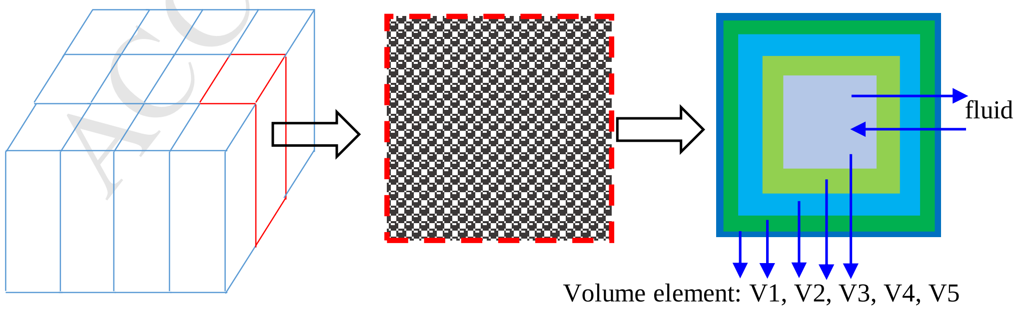

（1）matrix and natural fracture model

（2）MINC element

Figure 6. MINC model modified from Jiang and Younis [51]

③ In the third simulation case, the improved hybrid EDFM is used. The total grid number is 893 including 441 matrix grids, 441 natural fracture grids, and 11 hydraulic fracture cells. The pseudo-steady-state transfer between matrix and natural fracture is considered;

④ In the fourth simulation case, the improved hybrid EDFM is considered in which the transfer between matrix and natural fracture obeys transient flux model. The total grid number is 893.

The parameters used in the 2D synthetic model are shown in **Table 1**. The correlations for rock and fluid compressibility, viscosity and density can be found in the user manual of the commercial simulator Eclipse. The associated PVT data of dead oil (PVDO) are shown in **Table 2**. Then, we use eclipse to run the basic model. While the code of the framework programed by C++ is used for simulation cases 2, 3, and 4. The minimum time step is set to be equal to 0.1 day and the maximum time step is 30 days. The convergence criterion is set to be the summation of all calculation domain $\sum(\delta p, \delta S)^2$ in each newton iteration step. A simple time-stepping update strategy is employed: if the Newton method fails to converge, time step is reduced by half until it converges, while the maximum newton iteration step number should be less than 20.

Table 1. Specific of the base model

Parameter	Value	Unit
Reservoir length (NX/NY)	100 / 100	m
Formation thickness	10	m
Initial pressure	20	10^6 Pa
Initial Matrix Porosity	0.1	
Initial Naturally Fracture Porosity	0.00004	
Initial Hydraulic Fracture Porosity	1	
Rock compressibility	0.000855	10^{-6} Pa^{-1}
Rock reference pressure	20	10^6 Pa
Oil reference density	1000	kg/m^3
Natural Fracture aperture	2.00×10^{-04}	m
Matrix permeability	1.00×10^{-19}	m^2
Natural Fracture permeability	3.33×10^{-09}	m^2
Hydraulic Fracture aperture	1.00×10^{-03}	m
Hydraulic Fracture permeability	8.33×10^{-08}	m^2
Production BHP	8	10^6 Pa

Total simulation time	500	day [86400 s]

Figure 7 shows the oil production rates computed from four different models. As can been seen, the first simulation case, the second simulation case, and the fourth model are identical. We define the CPU time ratio as the simulation time of each case divided by the simulation time of the third case. The second simulation case shows significant difference with other three simulation models. In the simulation cases, the natural fracture permeability is $3330000\times10^{-15}m^2$ (the equivalent permeability is $66.6\times10^{-15}m^2$). The model proposed has the same accuracy compared with the LGR model and EDFM-MINC model. While the CPU time is much lower compared with the EDFM-MINC model. Here, the simulation time for LGR model was not presented because it runs with Eclipse and not use the program we develop. Actually, the CPU time is much longer than the other three simulation cases for the scenario with large Jacobian Matrix size. For the third simulation case, the CPU time is lower than other cases but it cannot keep a good accuracy. At the early production stage, the production rate generated from the third model is lower than those computed from the other three models, while at the late production stage, the production rate is higher. It can be seen that it is not reasonable to employ the pseudo steady state shape factor when the matrix is tight.

Table 2. PVT data of dead oil (part of data referring to Jiang and Younis [11])

Pressure (10^6 Pa)	**FVF**	**Viscosity(10^{-3} Pa·s)**
2.76	1.012	1.06
8.27	1.004	1.064
13.79	0.996	1.067
19.30	0.988	1.072
24.82	0.9802	1.077
30.34	0.9724	1.081
35.85	0.9646	1.085
38.61	0.9607	1.09

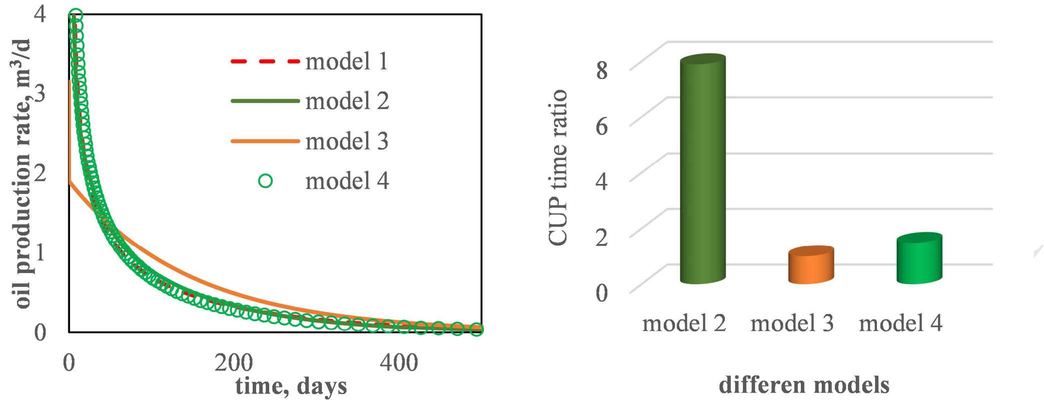

Figure 7. Oil production rate of four different models and CUP time ratio of three hybrid model

Next, we change the natural facture permeability to be $1000 \times 10^{-15} m^2$ (the equivalent permeability is $0.02 \times 10^{-15} m^2$) and run four simulation cases again. The production rate and CUP time ratio are shown in **Figure 8**. As can be seen, when the natural fracture has a relatively low conductivity, the new model can keep accuracy compared with the LGR model and EDFM+MINC model. **Figure 9** shows the iteration number of three hybrid models. As can been seen, the new hybrid model considering transient transfer between matrix and natural facture takes more iteration number than other two simulation models. Though the EDFM+MINC model costs the most time, the iteration number is not the highest. Thus, most time is consumed to solve the linear equation system for EDFM+MINC model.

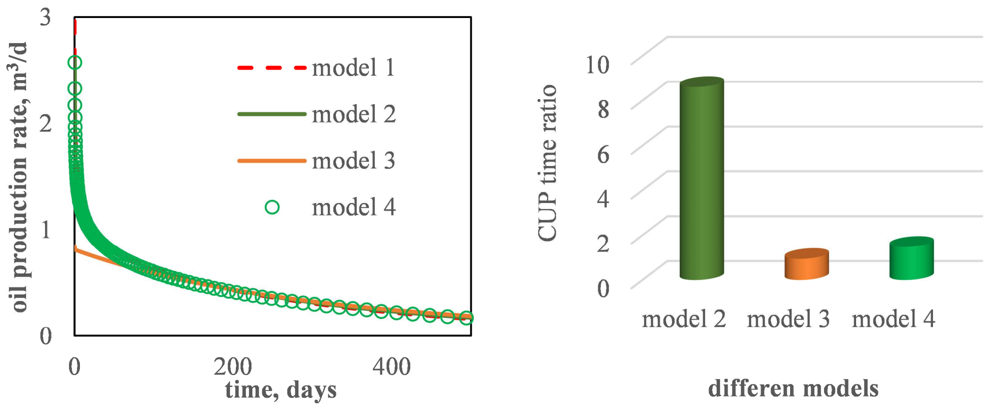

Figure 8. Oil production rate of four different models and CPU time ratio of three hybrid model

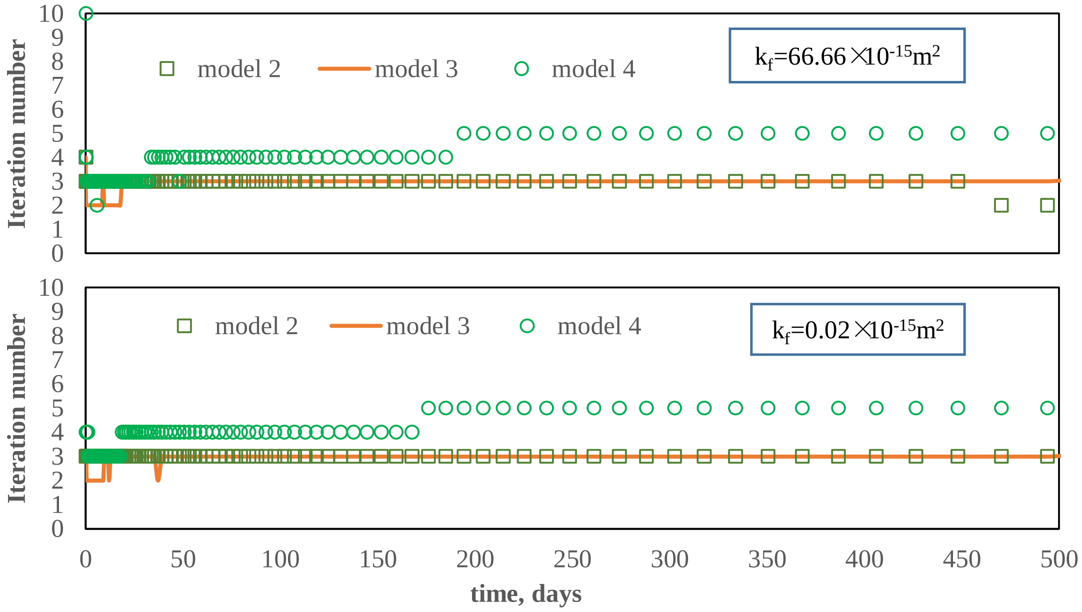

Figure 9. Iteration number in each time step of three hybrid models

5. Case study

5.1 Multistage fractured horizontal well

Figure 10 shows the geological model of a multistage fractured horizontal well. Three hydraulic fractures exist in the middle of the reservoir. Also, 20 large scale natural fractures distribute in the reservoir. The hydraulic fracture and large scale natural factures are modeled with EDFM method. The small scale natural factures are modeled with improved hybrid EDFM considering transient transfer. The reservoir is 310 m both in x and y directions. The grids are in according with **Figure 10**. Other basic parameters refer to **Table 1**.

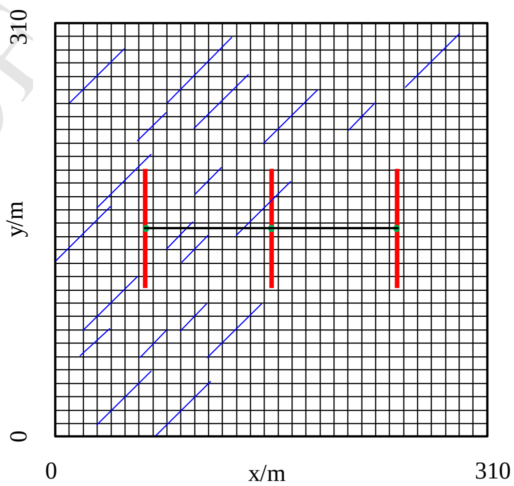

Figure 10. Geological model for case 1

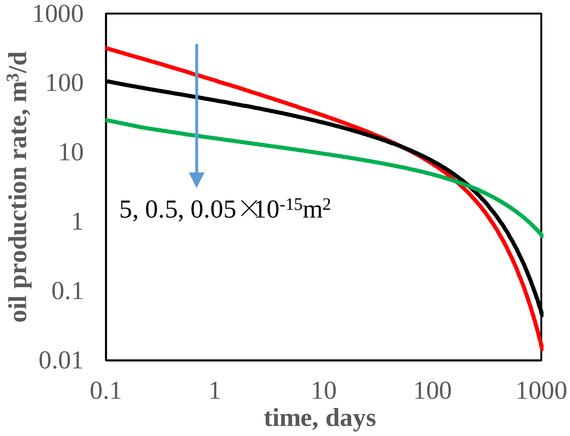

Figure 11. Effect of natural fracture permeability

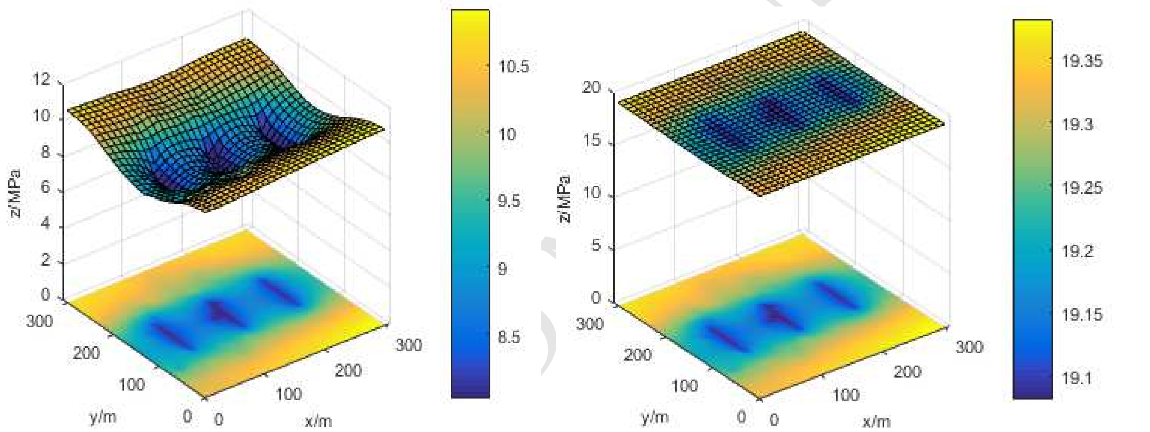

1 day (Left: natural fracture   Right:matrix)

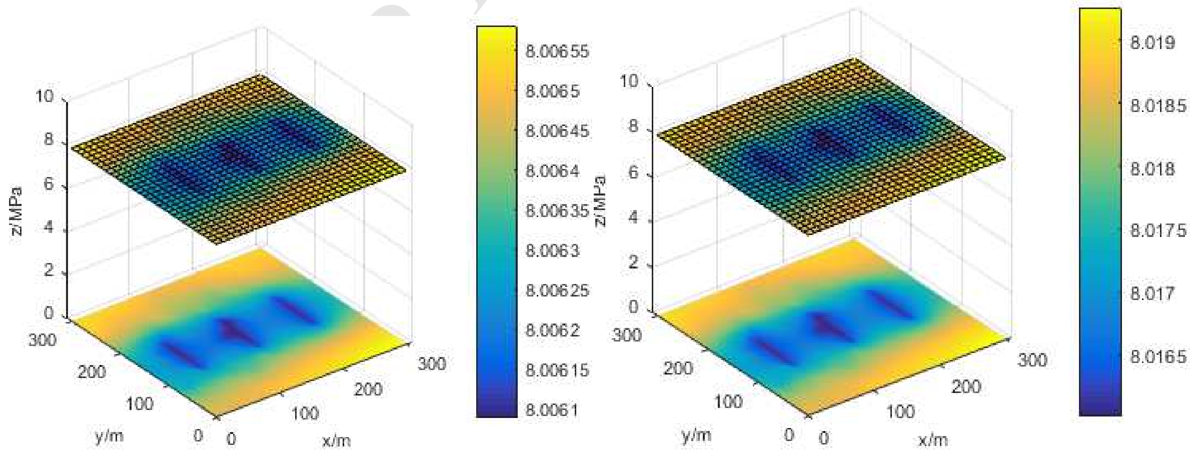

1000 day(Left: natural fracture   Right:matrix)

(1) Pressure distribution of natural fracture and matrix when k_f=5 $\times 10^{-15}$m^2

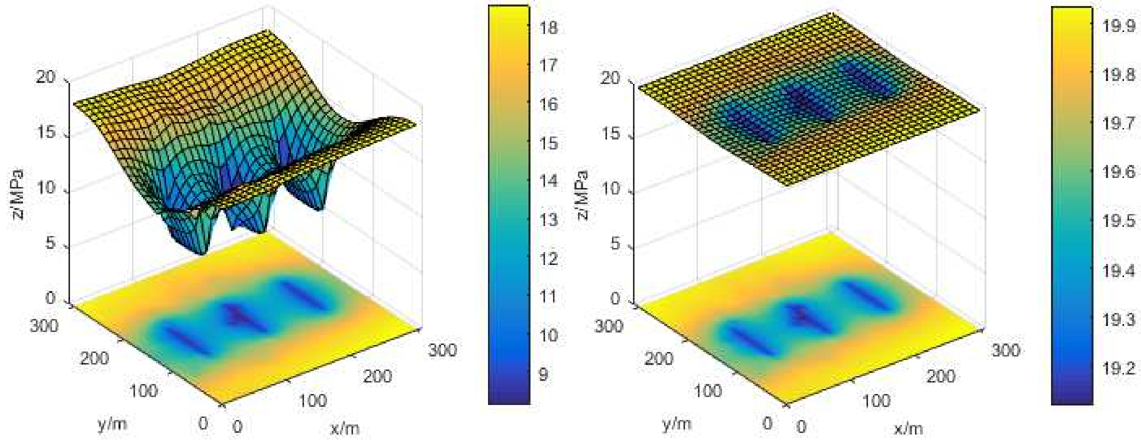

1 day(Left: natural fracture Right:matrix)

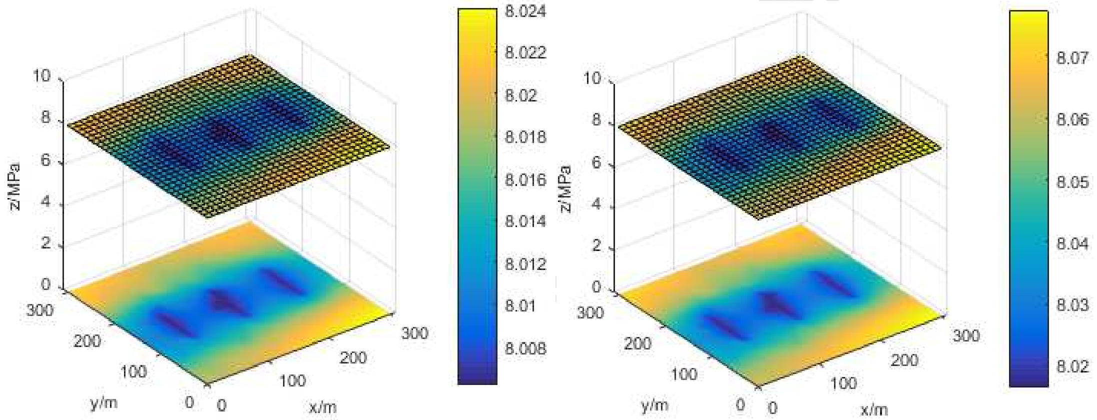

1000 day(Left: natural fracture Right:matrix)

(2) Pressure distribution of natural fracture and matrix when k_f=0.5 $\times 10^{-15}$m^2

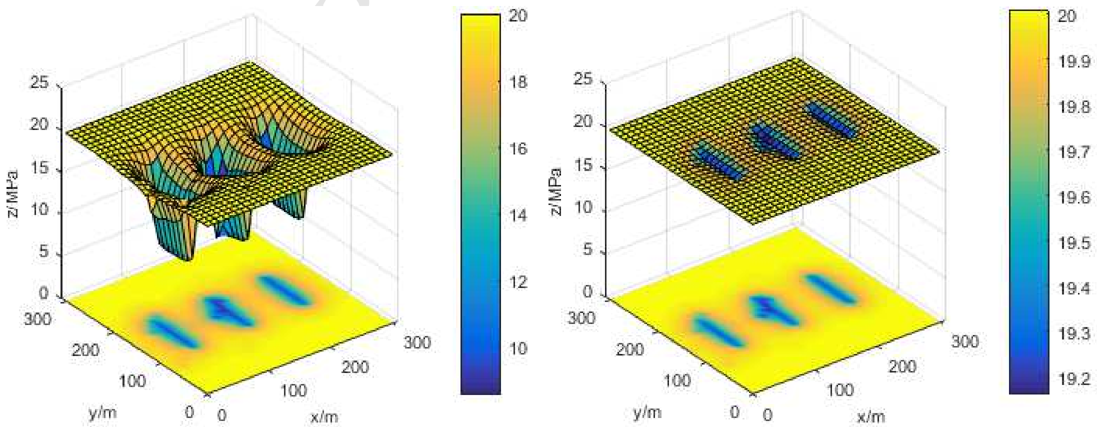

1 day(Left: natural fracture Right:matrix)

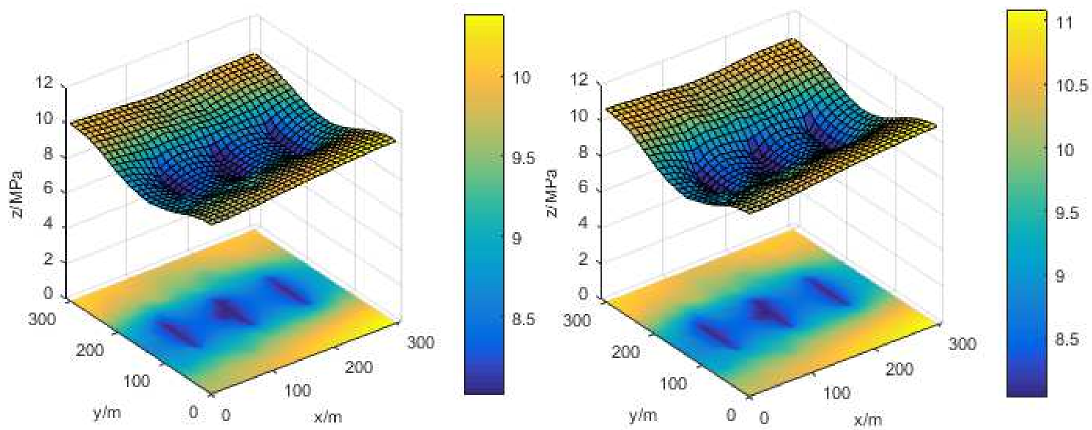

1000 day(Left: natural fracture Right:matrix)

(3) Pressure distribution of natural fracture and matrix when k_f=0.05×10^{-15}m^2

Figure 12. Pressure distribution of different models

Figure 11 shows the effect of natural fracture permeability on production performance. The natural fracture equivalent permeability is set to be 5×10^{-15}m^2, 0.5×10^{-15}m^2 and 0.05×10^{-15}m^2. With the natural fracture permeability equal to 5×10^{-15}m^2, the oil production rate is high at the early time. At the late time, oil production rate becomes the lowest when natural fracture permeability is equal to 5×10^{-15}m^2. Large natural fracture conductivity makes it easy to produce oil in the early time by decreasing the flow resistance.

Figure 12 shows the pressure distributions for the three models at different times. After 1 day's production, the natural fracture and matrix pressure decreases rapidly for the case when k_f=5 × 10^{-15}m^2. For the case with k_f=5×10^{-15}m^2, the natural fracture pressure drop is larger than the case with k_f=0.5×10^{-15}m^2. While for the case with k_f=0.05×10^{-15}m^2, the pressure spreads slowly and the pressure decrease is smaller than the former cases. A lot of regions in the reservoir keep the initial reservoir pressure both for natural fracture pressure and matrix pressure. Natural fracture permeability is a key parameter for the oil production rate at the early time. At the time of 1000 day, the reservoir pressure keeps higher for the case with k_f=0.05×10^{-15}m^2 than the other cases. The pressure spreads slowly, but the production rate is the highest at the late time stage. So it can be commented that natural facture permeability is beneficial for the rapid production of tight reservoir.

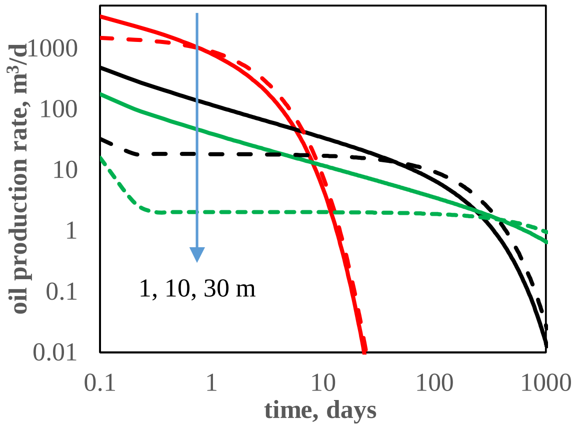

Figure 13. Effect of matrix size on production (dashed line: pseudo steady state transfer model; solid line: transient transfer model)

Figure 13 shows the effect of matrix size on oil production. Three matrix sizes are set to be as: L_x=L_y=1, 10, 30 m and L_z=10 m. The transient transfer and pseudo steady state transfer between matrix and natural fracture are both considered. As can been seen, the matrix size has great effect on oil production rate. The early production rate is high when matrix size is small, while at later time the rate is low. When L_x=L_y=1, the difference between transient transfer and pseudo steady state transfer model is not large after 1 day. This is due to the fact that when matrix size is small, it costs short time to reach to the pseudo steady state between matrix and natural fracture. While when L_x=L_y=30, the difference is obvious at all production time between two transfer models. Large matrix size makes it difficult to the pseudo steady state and the unsteady transfer will last longer. So if matrix size is big, error will happen using the pseudo steady transfer model.

Figure 14 shows the effect of matrix permeability on oil production. The matrix permeability is set to be 0.1, 0.001, 0.00001×10^{-15}m^2. When matrix permeability equals to 0.00001×10^{-15}m^2, oil production rate is small compared with other two cases at early time. The rates have big difference for the transient transfer and pseudo steady state transfer models. When k_m=0.1×10^{-15}m^2, oil rate is the biggest at the early time but declines rapidly. There is nearly no difference between the transient transfer and pseudo steady state transfer models for this case. This is because when the matrix permeability is big, it takes relatively short time to obtain pseudo steady state between matrix and natural fracture, while for a low permeability, time will last long for the transient transfer.

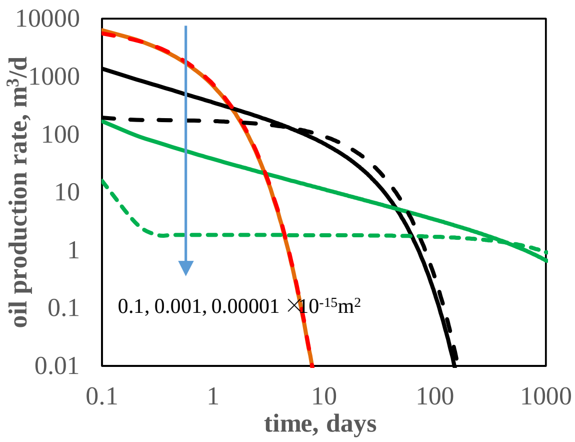

Figure 14. Effect of matrix permeability on production (dashed line: pseudo steady state transfer model; solid line: transient transfer model)

5.2 Complex hydraulic fracture

Table 3. Specific of the base model

Parameter	Value	Unit
Reservoir length (NX/NY)	310 / 310	m
Formation thickness	50	m
Initial pressure	24.8	10^6Pa
Initial Matrix Porosity	0.1	
Naturally Fracture Porosity	0.00001	
Hydraulic Fracture Porosity	1	
Rock compressibility	0.000855	10^{-6} Pa^{-1}
Water compressibility	0.0029	10^{-6} Pa^{-1}
Water viscosity compressibility Cvw	0.00018	10^{-6} Pa^{-1}
Water viscosity	0.54	10^{-3}Pa·s
Water Reference Pressure	24.8	10^6Pa
Water reference density	1000	kg/m^3
Water volume factor	1.00341	
Rock reference pressure	24.8	10^6Pa
Matrix size	L_x=L_y=10, L_z=50	m
Oil reference density	1000	kg/m^3
Hydraulic Fracture permeability	8.33×10^{-08}	m^2
Initial pressure	24.8	10^6Pa
Initial water saturation	0.3	
Production BHP	5.5	10^6Pa

Total simulation time	2000	day[86400 s]

Table 4. Relative permeability curve

Saturation	k_{rw}	k_{ro}
0	0	1
0.22	0.0484	0.98
0.3	0.09	0.4
0.4	0.16	0.125
0.6	0.36	0.0649
0.8	0.64	0.0048
0.9	0.83	0.001
1	1	0

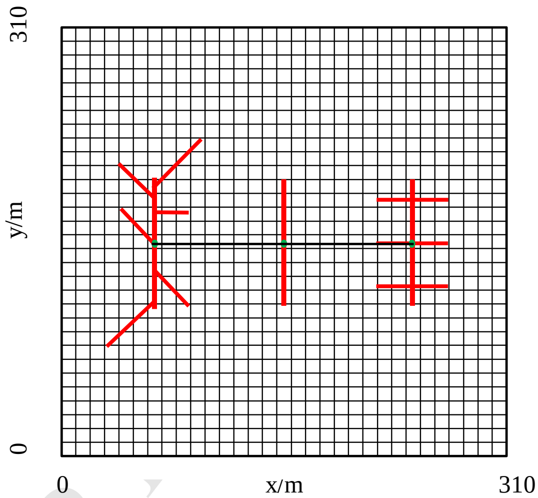

Figure 15. Geological model for complex hydraulic fracture

Figure 15 shows the geological model of a multistage horizontal well with complex hydraulic fractures. In this model, the two-phase flow is considered and the stochastic fracture and matrix permeability distribution are generated shown in **Figure 16.** The basis parameters refer to **Tables 2, 3,** and **4**. **Figure 16** Shows the permeability of natural fracture and matrix. The developed simulation workflow can be used in two-phase flow considering stochastic fracture permeability. **Figure 17** is the oil and water production rates of the transient transfer model and pseudo-steady-state transfer model. The water and oil rates have the same characteristics as the single phase flow. The hybrid simulation considering pseudo-steady-state transfer has a low production rate at early time. **Figure 18** shows the pressure distribution of different models at different times. As can been seen, the pressure first spreads around the hydraulic fractures. The stochastic fracture and matrix permeability affects the pressure spread in porous media. The zones with higher matrix permeability have a higher pressure decline.

6. Conclusion

In this paper, a new hybrid model combining the advantages of EDFM model and DP model for numerical simulation of tight oil reservoir is proposed and has been validated. The proposed model can be used for tight oil production analysis considering complex fracture networks. Some important conclusions are:

(1) The new hybrid simulation model considers the flow in matrix, natural fractures, and hydraulic fractures. Flow in three media are coupled with each other. The new hybrid simulation model employs the EDFM method to deal with large scale fractures while the natural fracture and matrix are modeled using dual porosity model.

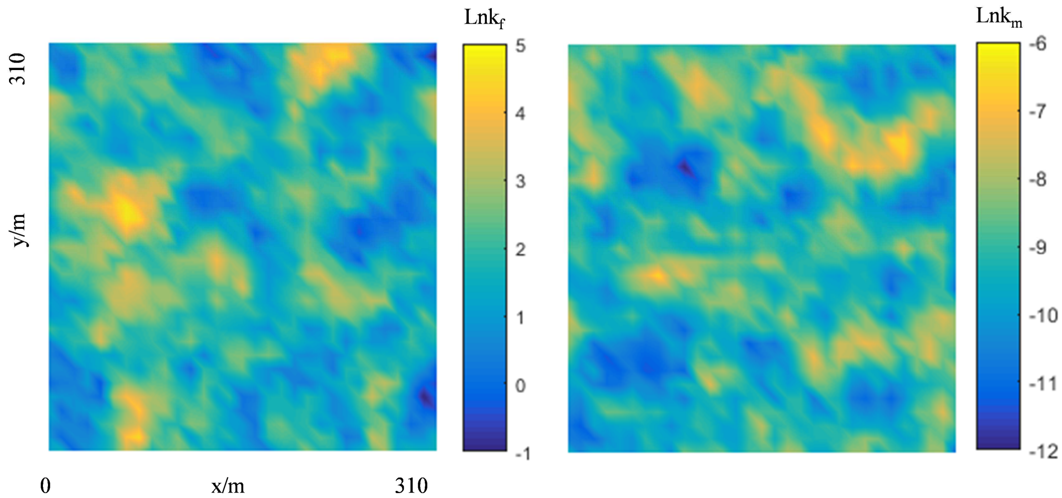

Figure 16 Stochastic fracture permeability and stochastic matrix permeability

(2) The model is verified by the case run and analysis of the well production rate. The new hybrid model with reasonable accuracy is computationally more efficient than EDFM-MINC model. The new model has decreased the calculation domains compared with EDFM-MINC. When considering pseudo steady state transfer between natural facture and matrix in production analysis for tight oil reservoir, the simulation results can lead to large error. The early production prediction rate is smaller than the real data and it has larger value in late time. The transient transfer model is more precise compared with the pseudo steady state transfer model. The LGR simulation results also indicated the transient transfer model is more reasonable.

(3) Matrix size and permeability has great effect on oil production. When the matrix size is small, the transient transfer between natural fracture and matrix lasts short. The difference between pseudo steady state transfer model and transient transfer model is relatively small. The early production rate is bigger when the matrix permeability is lager. While in the late production stage, the production rate is smaller. When the matrix permeability is bigger, the difference between transient transfer and pseudo steady state transfer becomes not obvious.

(4) The model can be used in both single phase and two-phase flow in tight oil reservoirs. Also, it can be used considering stochastic permeability. When considering two phases flow, the fluids (oil/water) production rates are different for transient transfer and pseudo steady state transfer model. The stochastic permeability makes the pressure distribution complex both for matrix and natural fracture.

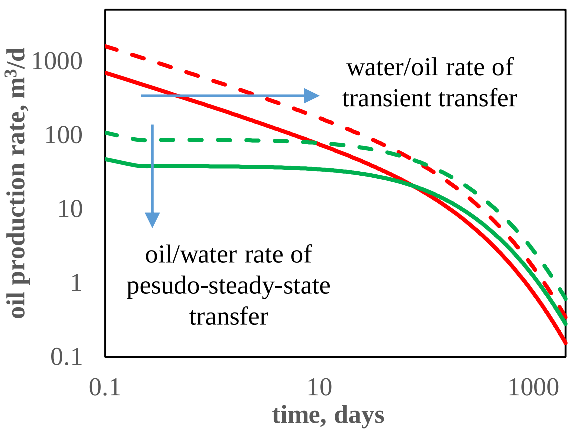

Figure 17. Production rate considering stochastic permeability

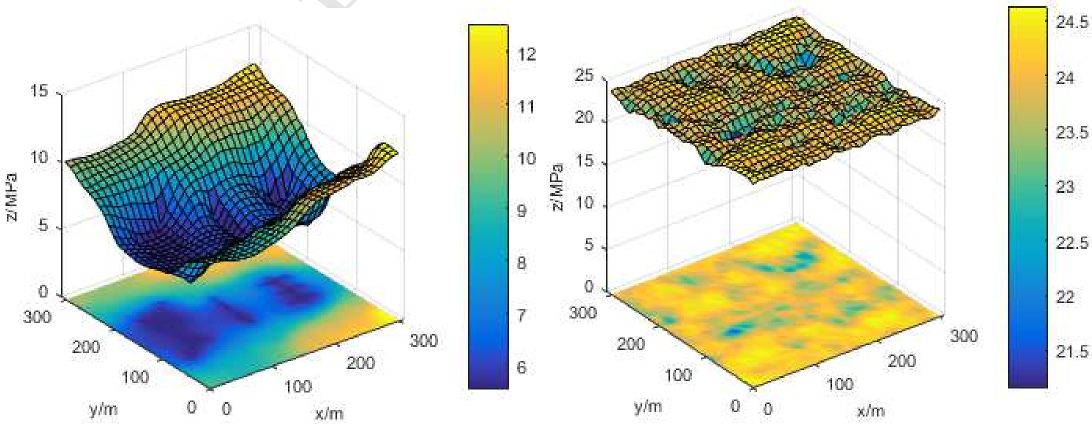

Transient transfer model after 1 day (Left: natural fracture; Right:matrix)

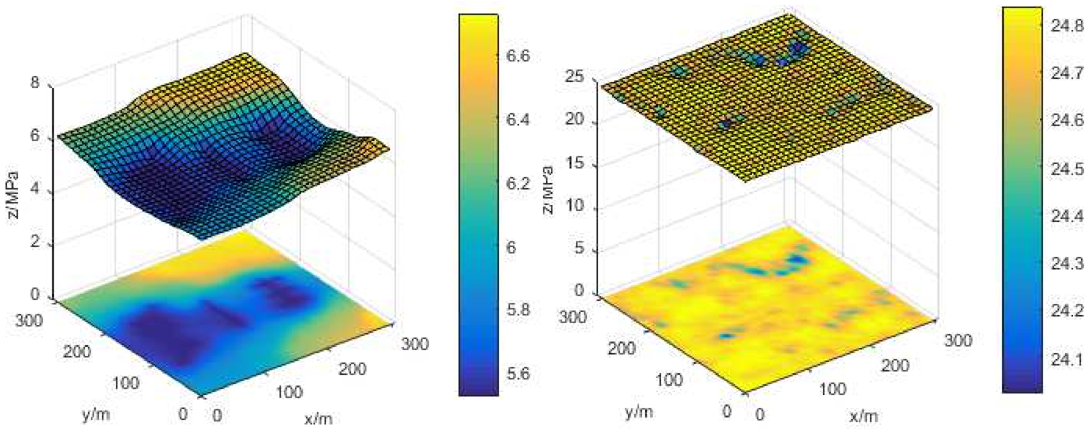

Pseudo steady state transfer model after 1 day (Left: natural fracture; Right:matrix)

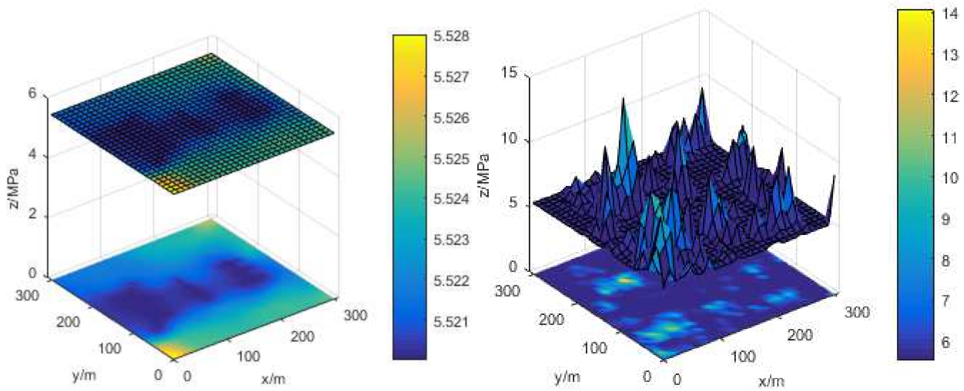

Transient transfer model after 2000 day (Left: natural fracture; Right:matrix)

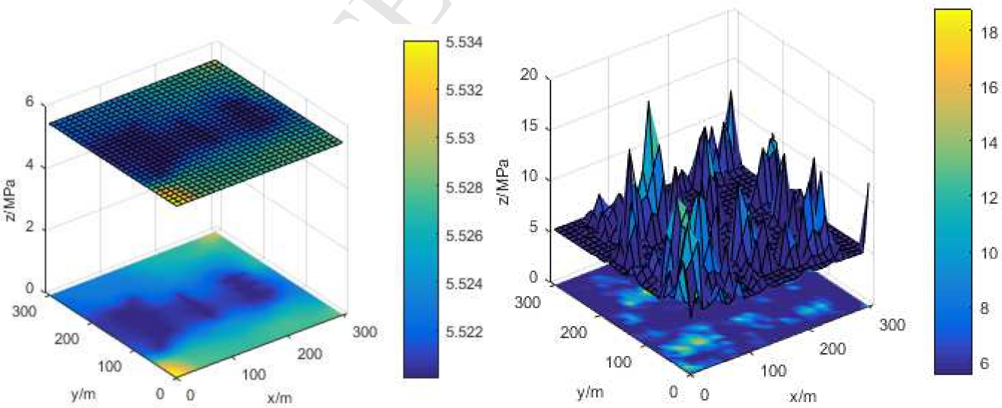

Pseudo steady state transfer model after 2000 day (Left: natural fracture; Right:matrix)

Figure 18. Pressure distribution of different models

Acknowledgement

This study was supported by the National Natural Science Foundation (U1762216), Natural Science Foundation of Shandong Province (ZR2016EEM30, JQ201716), the graduate innovation fund of China University of Petroleum (East China) under YCXJ2016018, and the Fundamental Research Funds for the Central University under 18CX02029A.

References

[1] Gao, J, & You, F. Design and optimization of shale gas energy systems: Overview, research challenges, and future directions. Computers & Chemical Engineering, 2017, 106: 699-718.

[2] Guerra, O J, Calderón, A J, Papageorgiou, L G, Siirola J J, & Reklaitis, G V. An optimization framework for the integration of water management and shale gas supply chain design. Computers & Chemical Engineering, 2016, 92: 230-255.

[3] Yang, S, Siddhamshetty, P, & Kwon, J S I. Optimal pumping schedule design to achieve a uniform proppant concentration level in hydraulic fracturing. Computers & Chemical Engineering, 2017, 101: 138-147.

[4] Guo, C, Xu, J, Wei, M, & Jiang, R. Experimental study and numerical simulation of hydraulic fracturing tight sandstone reservoirs. Fuel, 2015, 159: 334-344.

[5] Wang, L, Tian, Y, Yu, X, Wang, C, Yao, B, Wang, S, Winterfeld, P H, Wang, X, Yang, Z, Wang, Y, Cui, J, & Wu, Y. Advances in improved/enhanced oil recovery technologies for tight and shale reservoirs. Fuel, 2017, 210: 425-445.

[6] Zidane, A, & Firoozabadi, A. Fracture-cross-flow equilibrium in compositional two-phase reservoir simulation. SPE Journal, 2017, 22(03): 950-970.

[7] Barenblatt, G I, & Zheltov, Y P. Fundamental equations of filtration of homogeneous liquids in fissured rocks., Soviet Physics Doklady. 1960, 13: 545-548.

[8] Warren, J E, & Root, P J. The behavior of naturally fractured reservoirs. Society of Petroleum Engineers Journal, 1963, 3(03): 245-255.

[9] Kazemi, H, Merrill Jr, L S, Porterfield, K L, & Zeman, P R. Numerical simulation of water-oil flow in naturally fractured reservoirs. Society of Petroleum Engineers Journal, 1976, 16(06): 317-326.

[10] Thomas, L K, Dixon, T N, & Pierson, R G. Fractured reservoir simulation. Society of Petroleum Engineers Journal, 1983, 23(01): 42-54.

[11] Jiang, J, & Younis, R M. An improved projection-based embedded discrete fracture model

(pEDFM) for multiphase flow in fractured reservoirs. Advances in Water Resources, 2017, 109: 267-289.

[12] Steiner, C F, & Mittermeir, G M. Applicability of the shape-factor concept for naturally fractured reservoirs and an alternative approach. Journal of Petroleum Science and Engineering, 2017, 154: 60-75.

[13] Coats, K H. Implicit compositional simulation of single-porosity and dual-porosity reservoirs[C]//SPE Symposium on Reservoir Simulation. Society of Petroleum Engineers, 1989.

[14] Zimmerman, R W, Chen, G, Hadgu, T, & Bodvarsson, G S. A numerical dual□porosity model with semianalytical treatment of fracture/matrix flow. Water resources research, 1993, 29(7): 2127-2137.

[15] Kazemi, H, & Gilman, J R. Multiphase flow in fractured petroleum reservoirs[M]//Flow and Contaminant Transport in Fractured Rock. 1993, 31(91): 267-323.

[16] Lim, K T, & Aziz, K. Matrix-fracture transfer shape factors for dual-porosity simulators. Journal of Petroleum Science and Engineering, 1995, 13(3-4): 169-178.

[17] Hassanzadeh, H, & Pooladi-Darvish, M. Effects of fracture boundary conditions on matrix-fracture transfer shape factor. Transport in porous media, 2006, 64(1): 51-71.

[18] Hassanzadeh, H, Pooladi-Darvish, M, & Atabay, S. Shape factor in the drawdown solution for well testing of dual-porosity systems. Advances in water resources, 2009, 32(11): 1652-1663.

[19] Quintard, M, & Whitaker, S. Transport in chemically and mechanically heterogeneous porous media. I: Theoretical development of region-averaged equations for slightly compressible single-phase flow. Advances in Water Resources, 1996, 19(1): 29-47.

[20] Quintard, M, & Whitaker, S. Transport in chemically and mechanically heterogeneous porous media. II: Comparison with numerical experiments for slightly compressible single-phase flow. Advances in Water Resources, 1996, 19(1): 49-60.[21] Saboorian-Jooybari, H., Ashoori, S., & Mowazi G. Development of an analytical time-dependent matrix/fracture shape factor for countercurrent imbibition in simulation of fractured reservoirs. Transport in Porous Media, 2012, 92(3): 687-708.

[22] Sureshjani, M H, Gerami, S, & Emadi M A. Explicit rate–time solutions for modeling matrix–fracture flow of single phase gas in dual-porosity media. Transport in Porous Media, 2012, 93(1): 147-169.

[23] Ranjbar, E, Hassanzadeh, H, & Chen, Z. Semianalytical solutions for release of fluids from

rock matrix blocks with different shapes, sizes, and depletion regimes. Water Resources Research, 2013, 49(4): 2174-2196.

[24] Ranjbar, E, Hassanzadeh, H, & Chen, Z. Effect of fracture pressure depletion regimes on the dual-porosity shape factor for flow of compressible fluids in fractured porous media. Advances in Water Resources, 2011, 34(12): 1681-1693.

[25] Ranjbar, E, & Hassanzadeh, H. Matrix–fracture transfer shape factor for modeling flow of a compressible fluid in dual-porosity media. Advances in water resources, 2011, 34(5): 627-639.

[26] Rangel-German, E R, & Kovscek, A R. Time-dependent matrix-fracture shape factors for partially and completely immersed fractures. Journal of Petroleum Science and Engineering, 2006, 54(3): 149-163.

[27] He, Y, Chen, X, Zhang, Y, & Yu, W. Modeling interporosity flow functions and shape factors in low-permeability naturally fractured reservoir. Journal of Petroleum Science and Engineering, 2017, 156: 110-117.

[28] Bourbiaux, B, & Ding, D. Simulation of transient matrix-fracture transfers of compressible fluids. Transport in Porous Media, 2016, 114(3): 695-717.

[29] Azom, P N, & Javadpour, F. Dual-continuum modeling of shale and tight gas reservoirs[C]//SPE annual technical conference and exhibition. Society of Petroleum Engineers, 2012.

[30] Brown, M, Ozkan, E, Raghavan, R, & Kazemi, H. Practical solutions for pressure-transient responses of fractured horizontal wells in unconventional shale reservoirs. SPE Reservoir Evaluation & Engineering, 2011, 14(06): 663-676.

[31] Karimi-Fard, M, Durlofsky, L J, & Aziz, K. An efficient discrete-fracture model applicable for general purpose reservoir simulators. SPE Journal. 2004, 9 (2), 227–236.

[32] Monteagudo, J E P, & Firoozabadi, A. Control□volume method for numerical simulation of two□phase immiscible flow in two□and three□dimensional discrete□fractured media. Water resources research, 2004, 40(7).

[33] Zidane, A, & Firoozabadi, A. An efficient numerical model for multicomponent compressible flow in fractured porous media. Advances in Water Resources, 2014, 74: 127-147.

[34] Wang, Y, & Shahvali, M. Discrete fracture modeling using centroidal voronoi grid for simulation of shale gas plays with coupled nonlinear physics. Fuel, 2016, 163: 65-73.

[35] Li, D, Zhang, L, Wang, J Y, & Lu, D. Composition-transient analysis in shale-gas reservoirs

with consideration of multicomponent adsorption. SPE Journal, 2016, 21(02): 648-664.
[36] Li, D, Xu, C, Wang, J Y, & Lu, D. Effect of Knudsen diffusion and Langmuir adsorption on pressure transient response in tight-and shale-gas reservoirs. Journal of Petroleum Science and Engineering, 2014, 124: 146-154.
[37] Lee, S H, Lough, M F, & Jensen, C L. Hierarchical modeling of flow in naturally fractured formations with multiple length scales. Water Resources Research, 2001, 37(3): 443-455.
[38] Li, L, & Lee, S H. Efficient field-scale simulation of black oil in a naturally fractured reservoir through discrete fracture networks and homogenized media. SPE Reservoir Evaluation & Engineering, 2008, 11(4): 750-758.
[39] Moinfar, A, Narr, W, Hui, M H, Mallison, B T, & Lee, S H. Comparison of discrete-fracture and dual-permeability models for multiphase flow in naturally fractured reservoirs[C]//SPE Reservoir Simulation Symposium. Society of Petroleum Engineers, 2011.
[40] Moinfar, A, Varavei, A, Sepehrnoori, K, & Johns, R T. Development of a novel and computationally-efficient discrete-fracture model to study IOR processes in naturally fractured reservoirs[C]//SPE Improved Oil Recovery Symposium. Society of Petroleum Engineers, 2012.
[41] AlTwaijri, M, Xia, Z, Yu, W, Qu, L, Hu, Y, Xu, Y, & Sepehrnoori, K. Numerical study of complex fracture geometry effect on two-phase performance of shale-gas wells using the fast EDFM method. Journal of Petroleum Science and Engineering, 2018, 164: 603-622.
[42] de Araujo Cavalcante Filho, J S, & Sepehrnoori, K. Simulation of planar hydraulic fractures with variable conductivity using the embedded discrete fracture model. Journal of Petroleum Science and Engineering, 2017, 153: 212-222.
[43] Ren, G, Jiang, J, & Younis, R M. Fully Coupled Geomechanics and Reservoir Simulation for Naturally and Hydraulically Fractured Reservoirs[C]//50th US Rock Mechanics/Geomechanics Symposium. American Rock Mechanics Association, 2016.
[44] de Sousa Junior, L C, dos Santos, L O S, de Souza Rios, V, Araújo, C, Celes, W, & Sepehrnoori, K. Methodology for geomechanically controlled transmissibility through active natural fractures in reservoir simulation. Journal of Petroleum Science and Engineering, 2016, 147: 7-14.
[45] Norbeck, J H, McClure, M W, Lo, J W, & Horne, R N. An embedded fracture modeling framework for simulation of hydraulic fracturing and shear stimulation. Computational Geosciences, 2016, 20(1): 1-18.

[46] Siripatrachai, N, Ertekin, T, & Johns, R T. Compositional simulation of hydraulically fractured tight formation considering the effect of capillary pressure on phase behavior. SPE Journal, 2017, 22(04): 1046-1063.
[47] Zuloaga-Molero, P, Yu, W, Xu, Y, Sepehrnoori, K, & Li, B. Simulation Study of CO2-EOR in Tight Oil Reservoirs with Complex Fracture Geometries. Scientific reports, 2016, 6: 33445.
[48] Zhang, Y, Yu, W, Sepehrnoori, K, & Di, Y. A Comprehensive Numerical Model for Simulating Fluid Transport in Nanopores. Scientific reports, 2017, 7: 40507.
[49] Xu, Y, Cavalcante Filho, J S, Yu, W, & Sepehrnoori, K. Discrete-Fracture Modeling of Complex Hydraulic-Fracture Geometries in Reservoir Simulators. SPE Reservoir Evaluation & Engineering, 2017, 20(02): 403-422.
[50] Panfili, P, & Cominelli, A. Simulation of miscible gas injection in a fractured carbonate reservoir using an embedded discrete fracture model[C]//Abu Dhabi International Petroleum Exhibition and Conference. Society of Petroleum Engineers, 2014.
[51] Jiang, J, & Younis, R M. Hybrid coupled discrete-fracture/matrix and multicontinuum models for unconventional-reservoir simulation. SPE Journal, 2016, 21(03): 1,009-1,027.
[52] Chai, Z, Yan, B, Killough, J E, & Wang, Y. An Efficient Method for Fractured Shale Reservoir History Matching: The Embedded Discrete Fracture Multi-Continuum Approach[C]//SPE Annual Technical Conference and Exhibition. Society of Petroleum Engineers, 2016.
[53] Wang, K, Liu, H, Luo, J, Wu, K, & Chen, Z. A Comprehensive Model Coupling Embedded Discrete Fractures, Multiple Interacting Continua, and Geomechanics in Shale Gas Reservoirs with Multiscale Fractures. Energy & Fuels, 2017, 31(8): 7758-7776.
[54] Jiang, J, & Younis, R M. A multimechanistic multicontinuum model for simulating shale gas reservoir with complex fractured system. Fuel, 2015, 161: 333-344.
[55] Weng, X, Kresse, O, Chuprakov, D, Cohen, C E, Prioul, R, & Ganguly, U. Applying complex fracture model and integrated workflow in unconventional reservoirs. Journal of Petroleum Science and Engineering, 2014, 124: 468-483.
[56] Longo, S, & Di Federico, V. Unsteady flow of shear-thinning fluids in porous media with pressure-dependent properties. Transport in Porous Media, 2015, 110(3): 429-447.
[57] Di Federico, V, Longo, S, King, S E, Chiapponi, L, Petrolo, D, & Ciriello, V. Gravity-driven flow of Herschel–Bulkley fluid in a fracture and in a 2D porous medium. Journal of Fluid

Mechanics, 2017, 821: 59-84.
[58] Mayerhofer, M J, Lolon, E, Warpinski, N R, Cipolla, C L, Walser, D W, & Rightmire, C M. What is stimulated reservoir volume?. SPE Production & Operations, 2010, 25(01): 89-98.
[59] Chen Z, Huan G, & Li B. Modeling 2D and 3D horizontal wells using CVFA. Communications in Mathematical Sciences, 2003, 1(1): 30-43.

Highlights

► Established the hybrid numerical simulation method of naturally fractured tight oil reservoir.

► Coupled the EDFM and DP model considering transient transfer firstly.

► Validated the new model compared with some existing models.

► Effect of relevant parameters was modeled and analyzed.

► The new method has high calculation efficiency and good accuracy.